





A Dynamical Model of the M101/NGC 5474 Encounter

Sean T. Linden¹  and J. Christopher Mihos² ¹Department of Astronomy, University of Massachusetts at Amherst, Amherst, MA 01003, USA²Department of Astronomy, Case Western Reserve University, Cleveland OH 44106, USA

Received 2022 May 31; revised 2022 June 23; accepted 2022 June 24; published 2022 July 11

Abstract

We present the first dynamical simulation that recreates the major properties of the archetypal nearby spiral galaxy M101. Our model describes a grazing but relatively close (~ 14 kpc) passage of the companion galaxy NGC 5474 through M101's outer disk approximately 200 Myr ago. The passage is retrograde for both disks, yielding a relatively strong gravitational response while suppressing the formation of long tidal tails. The simulation reproduces M101's overall lopsidedness, as well as the extended NE Plume and the sharp western edge of the galaxy's disk. The post-starburst populations observed in M101's NE Plume are likely a result of star formation triggered at the point of contact where the galaxies collided. Over time, this material will mix azimuthally, leaving behind diffuse, kinematically coherent stellar streams in M101's outer disk. At late times after the encounter, the density profile of M101's disk shows a broken "upbending" profile similar to those seen in spiral galaxies in denser environments, further demonstrating the connection between interactions and long-term structural changes in galaxy disks.

Unified Astronomy Thesaurus concepts: [Galaxy interactions \(600\)](#); [Galaxy evolution \(594\)](#); [Galaxy dynamics \(591\)](#)

Supporting material: animations

1. Introduction

Due to its proximity and large angular size, the spiral galaxy M101 is one of the most well-studied galaxies in the sky, yielding important information on the dynamics of spiral structure, the interplay between ISM physics and star formation, and the formation and evolution of stars and stellar populations. However, M101's strong global asymmetry and complex H I kinematics (e.g., Waller et al. 1997; Walter et al. 2008; Mihos et al. 2012, 2013) show that the galaxy is not in dynamical equilibrium, complicating its use as a template for studying the physical processes at work in galaxy disks.

While interactions in the group environment have clearly shaped M101's recent history (e.g., Waller et al. 1997), the details are poorly constrained, and even the main interaction partner remains unclear. The dwarf galaxy NGC 5477 lies near the edge of M101's disk but is likely too low in mass to drive M101's highly asymmetric HI structure. Meanwhile, the brighter companion NGC 5474 is projected ~ 90 kpc to the southeast, and while the galaxy shows an off-center bulge, its disk is otherwise normal kinematically and morphologically (Rownd et al. 1994). No detailed model exists describing M101's interaction history, and this uncertainty makes it hard to link the dynamical conditions in the galaxy to the properties of its ISM and existing stellar populations.

However, recent data have provided new constraints on our understanding of the M101 system. Deep imaging of M101's outer disk has revealed additional signatures of recent interaction, including the extended NE Plume and E Spur (Mihos et al. 2013), but no evidence for long tidal tails or connecting tidal bridges between M101 and any of its

companions. Meanwhile, Hubble imaging of the stellar populations in M101's NE Plume has revealed ~ 300 Myr old post-starburst population (Mihos et al. 2018), likely marking the time since M101's most recent interaction. These observations, coupled with deep H I mapping of the M101 system (Walter et al. 2008; Mihos et al. 2012; Xu et al. 2021) and new imaging and spectroscopy of NGC 5474 (Bellazzini et al. 2020), provide updated constraints on a potential interaction between M101 and NGC 5474. We use these new constraints to develop the first self-consistent N -body simulation of the M101/NGC 5474 encounter, explaining a wide variety of the observed properties while also giving insight into the subsequent evolution of M101's disk. Given M101's important role as a template for studying the detailed physical processes governing disk evolution, ISM physics, and star formation in spiral galaxies, as well as its status as the dominant spiral in a galaxy group (Geller & Huchra 1983; Tully 1988), this simulation sets the stage not only for a better understanding of M101 specifically but more generally for spiral galaxies and their evolution in group environments.

2. Simulation Methods

While the focus of this study is the interaction between M101 and its companion galaxy NGC 5474, in a preliminary set of models we also examined the effects of M101's smaller companion, NGC 5477. We ran simulations involving low-mass companions ($M_{\text{NGC 5477}}/M_{\text{M101}} = 0.01$, comparable to the B -band luminosity ratio of the galaxies) on a variety of circular and elliptical orbits chosen to match the 44 kpc projected separation of the pair. While these simulations showed a propensity to drive symmetric two-armed spiral modes in M101, none were successful in reproducing M101's strong $m = 1$ disk asymmetry or the observed tidal morphology of its outer disk. These outcomes led us to turn to simulations involving a stronger fly-by encounter between M101 and the



Original content from this work may be used under the terms of the [Creative Commons Attribution 4.0 licence](#). Any further distribution of this work must maintain attribution to the author(s) and the title of the work, journal citation and DOI.

more distant and more massive companion NGC 5474, described below.

To build our N -body galaxy models of M101 and NGC 5474, we follow the method of Hernquist (1993), wherein each galaxy consists of a stellar disk, a surrounding dark matter halo, and, in the case of the NGC 5474 model, a central bulge. We omit the bulge component in the M101 model due to the galaxy’s extremely low bulge:disk ratio (e.g., Kormendy et al. 2010). The disks follow an exponential density profile, while both the dark halos and the NGC 5474 bulge follow a spherical Hernquist (1990) model:

$$\rho(r) = \frac{M a}{2\pi r (r + a)^3}.$$

We set the halo scale radius (a_h) for the M101 model to be 10 times the disk scale length and, for computational expediency, truncate the dark halo beyond 100 disk scale lengths. The disk:halo mass ratio of the M101 model is 1:23, and we set the circular velocity and disk scale length of the M101 model to match M101’s observed properties ($V_{c,M101} = 220 \text{ km s}^{-1}$ and $h_{R,M101} = 4.4 \text{ kpc}$; Bosma et al. 1981; Mihos et al. 2013, respectively). This yields a total disk mass of $M_{\text{disk}} = 5.3 \times 10^{10} M_{\odot}$ and gives the model a slowly rising rotation curve that flattens at large radius.

We build the NGC 5474 model in a similar fashion, setting its disk scale length to $h_{R,N5474} = 1.5 \text{ kpc}$ and adding a central bulge with a bulge:disk mass ratio of 1:3, in rough accordance with the observed properties of the system (e.g., Bellazzini et al. 2020). However, in reality, NGC 5474’s bulge is strangely offset from the center of its disk by $\sim 1 \text{ kpc}$ (e.g., Rownd et al. 1994; Pascale et al. 2021), suggesting the galaxy is likely well out of equilibrium, and our attempts to match the observed kinematics of the galaxy proved problematic. Scaling our galaxy model in mass to match NGC 5474’s observed circular velocity (40 km s^{-1} ; Rownd et al. 1994) gives a total (disk+bulge+halo) mass of $2.5 \times 10^{10} M_{\odot}$ and a mass ratio of the M101/NGC 5474 system of $\approx 35:1$. However, in preliminary models at this mass ratio, we found NGC 5474 to be too low in mass to drive the strong asymmetric response seen in M101’s disk. Instead, we were pushed to a higher mass for the companion, ultimately adopting an 8:1 mass ratio for the galaxy pair, which yielded a significantly higher circular velocity for NGC 5474 of 135 km s^{-1} . This mass discrepancy remains one shortcoming of our model, but we note that recent simulations of NGC 5474 by Pascale et al. (2021) that try to match both the morphology and kinematics of this galaxy suggest that NGC 5474’s bulge and disk may in fact be two separate and interacting galaxies themselves. Given the surprisingly complex nature of this galaxy and its uncertain dynamical state, we choose to focus our modeling efforts largely on M101’s response and leave the NGC 5474 discrepancy for future follow-up studies.

Our primary goal in designing the encounter model was to reproduce the large-scale morphology and kinematics of M101: the galaxy’s strong $m = 1$ lopsidedness, its extended NE Plume, and the sharp edge to the western side of its disk (Mihos et al. 2013). These are all gravitational effects, so for simplicity our simulations are purely collisionless and do not model the hydrodynamic evolution of the interstellar medium or the star-forming response of the disk. We evolve the simulations using the hierarchical treecode of Hernquist (1987), with a fixed time

step of 0.68 Myr and using a total of 1,00,000 and 165,000 particles to model M101 and NGC 5474, respectively.

Aside from the morphological constraints, our simulations are also constrained by the projected relative positions and velocities of the galaxies. These various considerations led to limitations on the orbital geometries of the disks (disk inclinations i and arguments of periaapse ω ; see Toomre & Toomre 1972) and the viewing angle of the system. The small difference in systemic velocity (30 km s^{-1}) led us to focus on orbits that occurred largely in the sky plane to minimize the projected orbital velocity. Because M101 and NGC 5474 are both observed mostly face on, this argument in turn implied highly prograde or retrograde orbits ($i \sim 0^\circ$ or 180°), rather than polar encounters ($i \sim 90^\circ$). In our initial modeling tests, we found that prograde encounters strong enough to drive the observed M101 asymmetry also resulted in long tidal tails, which are not observed in the system. These tests also showed that the resulting lopsidedness of M101’s disk was a strong function of pericenter distance, while M101’s argument of periaapse ω was limited to a small range due to the need to match the current projected location of NGC 5474 relative to M101. All these considerations ultimately led us to favor the dual retrograde encounter described below.

3. Best-match Interaction Scenario

Our best-match simulation begins with NGC 5474 located 175 kpc away from M101, moving on a parabolic orbit initialized as Keplerian with a 4.4 kpc pericenter distance. However, due to the galaxies’ extended halo mass distributions, the orbital track deviates from this idealized orbit, and the galaxies reach a much wider periaapse of 13.7 kpc. The orientation of both disks is primarily retrograde, with inclinations and arguments of periaapse given by $(i, \omega)_{M101} = (195^\circ, 265^\circ)$ and $(i, \omega)_{N5474} = (150^\circ, 100^\circ)$. The system is viewed with the orbit plane slightly inclined by $\sim 10^\circ$ from the sky plane ($\sim 15^\circ$ from M101’s disk plane).³

As the interaction proceeds (Figure 1), NGC 5474 enters from the north, passing through the west side of M101’s outer disk approximately 200 Myr ago. Material on the side of the disk near the impact point feels a dispersive impulse and is scattered outwards, eventually rotating around the galaxy to be seen today as the NE Plume. Meanwhile, the passage of the companion pulls M101 westward, leading to crowding and compression of material along the disk’s current western edge. The interaction is not so strong as to lead to a merger; NGC 5474 exits to the southeast and continues to move away from M101 today. Viewed edge on to the sky plane (Figure 2), we see the oblique nature of the encounter. NGC 5474 skims through M101’s outer disk at a shallow 15° angle, scattering material near the contact point vertically out of the disk plane. This leads to a flaring of M101’s outer disk, with material currently in the NE Plume moving away along our line of sight (i.e., “behind” M101’s disk plane from our perspective).

The simulation reproduces much of the morphology of the M101 system, including the lopsidedness of the inner disk, the extended NE Plume, and the sharp isophotal cutoff on the disk’s western edge. M101’s prominent NE arm can be seen developing shortly after the initial impact, then swinging around to its current location; we also see a broken dog-leg

³ Additional simulation details, particle snapshot files, and visualizations are available at <http://astroweb.case.edu/hos/M101Sim>.

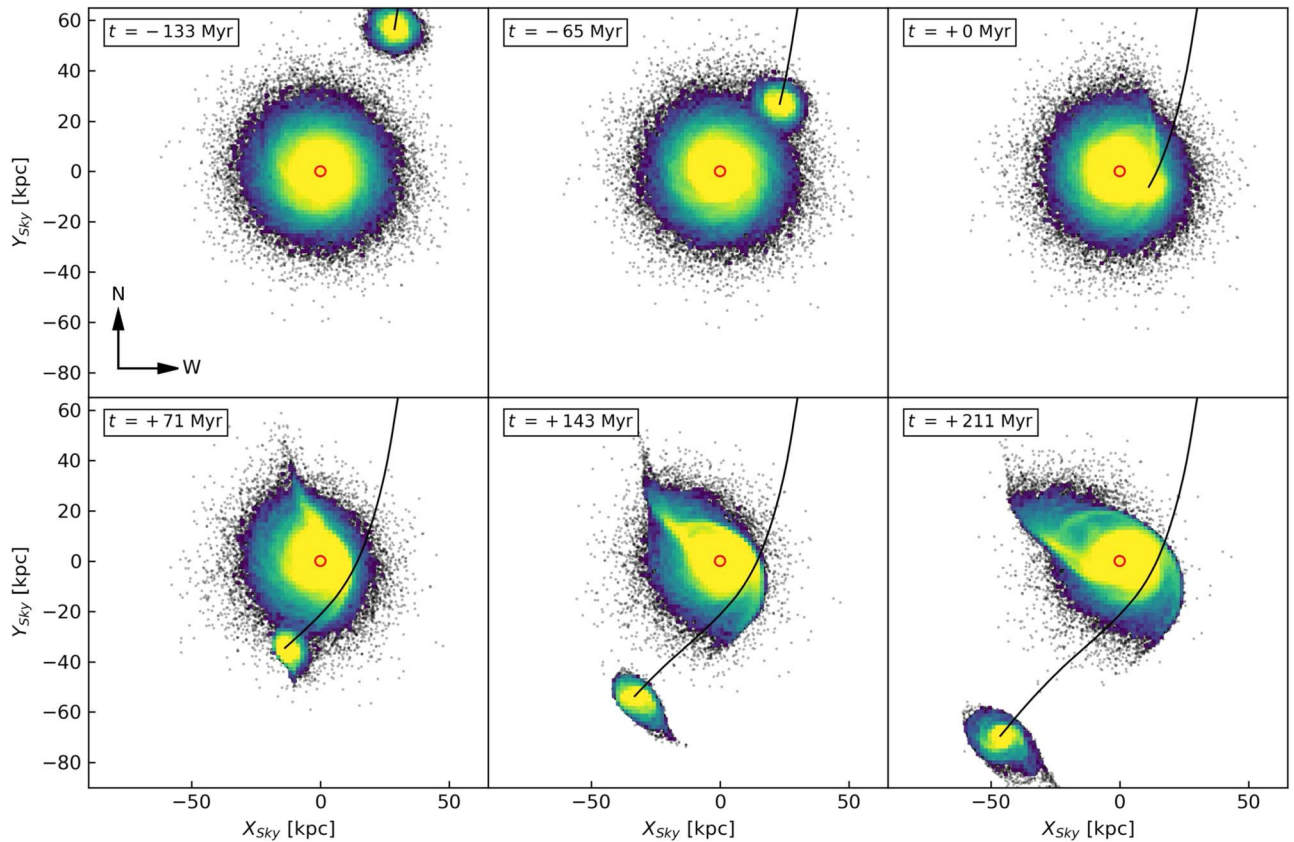


Figure 1. Sky view of the M101/NGC 5474 encounter. Time is measured relative to the moment of periape ($t = 0$), with the last panel showing the current time. The red circle shows a 2 kpc radius centered on M101’s nucleus. The simulation is visualized using a frame of reference that fixes M101 at the origin at all times, and NGC 5474’s orbital track is shown by the black line. An animation of this figure is available, showing the evolution of the interaction from $t = -269$ Myr to $t = +374$ Myr. The real-time duration of the animation is 24 s, and the animation pauses for 5 s at $t = +211$ Myr, the time of best match to the present-day M101/NGC 5474 system.

(An animation of this figure is available.)

structure that bends the arm to the northwest, similar to that observed in M101 itself (see Figure 4). The relative position and velocity of NGC 5474 is reproduced well, while the dual retrograde geometry explains the lack of long tidal tails around either galaxy.

Of particular interest is the history of the NE Plume. Its very blue integrated colors led Mihos et al. (2013) to propose a recent weak burst of star formation in the region. This was recently confirmed by deep Hubble Space Telescope imaging (Mihos et al. 2018), which revealed the presence of ~ 300 Myr old post-starburst stellar populations in the Plume. According to our simulation, material in today’s NE Plume was originally at the contact point where NGC 5474 passed through M101’s disk, as shown in Figure 3. As NGC 5474 approaches M101, compressive tidal forces should lead to an increase in the turbulent energy and the velocity dispersion of the ISM. Hydrodynamical simulations of starburst activity in galaxy mergers suggest that the kinetic energy carried by compressive turbulence, and the subsequent increase in the dense gas fraction in the ISM, begins as early as ~ 50 Myr before closest approach (Renaud et al. 2014, 2018). Indeed, in our own simulations shown here, an analysis of the local velocity field in M101’s outer disk near the collision point shows signatures of convergent velocity 25–50 Myr before the moment of periape, as the companion comes in contact with M101’s disk (see also Renaud et al. 2009). While our collisionless simulation precludes us from following the hydrodynamical

response of the ISM, the enhanced turbulence driven by these compressive effects likely generates an excess of dense gas at this location, triggering the starburst episode recorded in the NE Plume’s stellar populations. Therefore, depending on the early response of the star-forming gas, we might expect to see differences of 50 Myr between the ~ 300 Myr old stellar population age in the Plume and the ~ 200 Myr time since periape in our simulation, which partially explain these slightly discrepant timescales. These details aside, the dynamical connection between the Plume’s post-starburst stellar population and star formation triggered at the original impact site is plausibly demonstrated in our model.

Deep imaging of M101’s outer disk has also revealed a second tidal feature, the fainter and redder “Eastern Spur” (Mihos et al. 2013), extending from the SE side of M101’s disk. While our simulation shows no distinct feature here, the material on this side of the disk was originally on the north side of M101 and moving away from NGC 5474 when the companion passed through M101’s disk. Thus, this material felt a much weaker perturbation, likely explaining its redder colors, lack of induced star formation, and more passive evolution.

Our simulation also captures the observed kinematics of the M101/NGC 5474 system quite well. Figure 4 shows position–velocity plots of the simulation viewed at the best-match time, where it can be seen that NGC 5474 has a small $+20 \text{ km s}^{-1}$ redshift relative to M101, similar to the observed value of

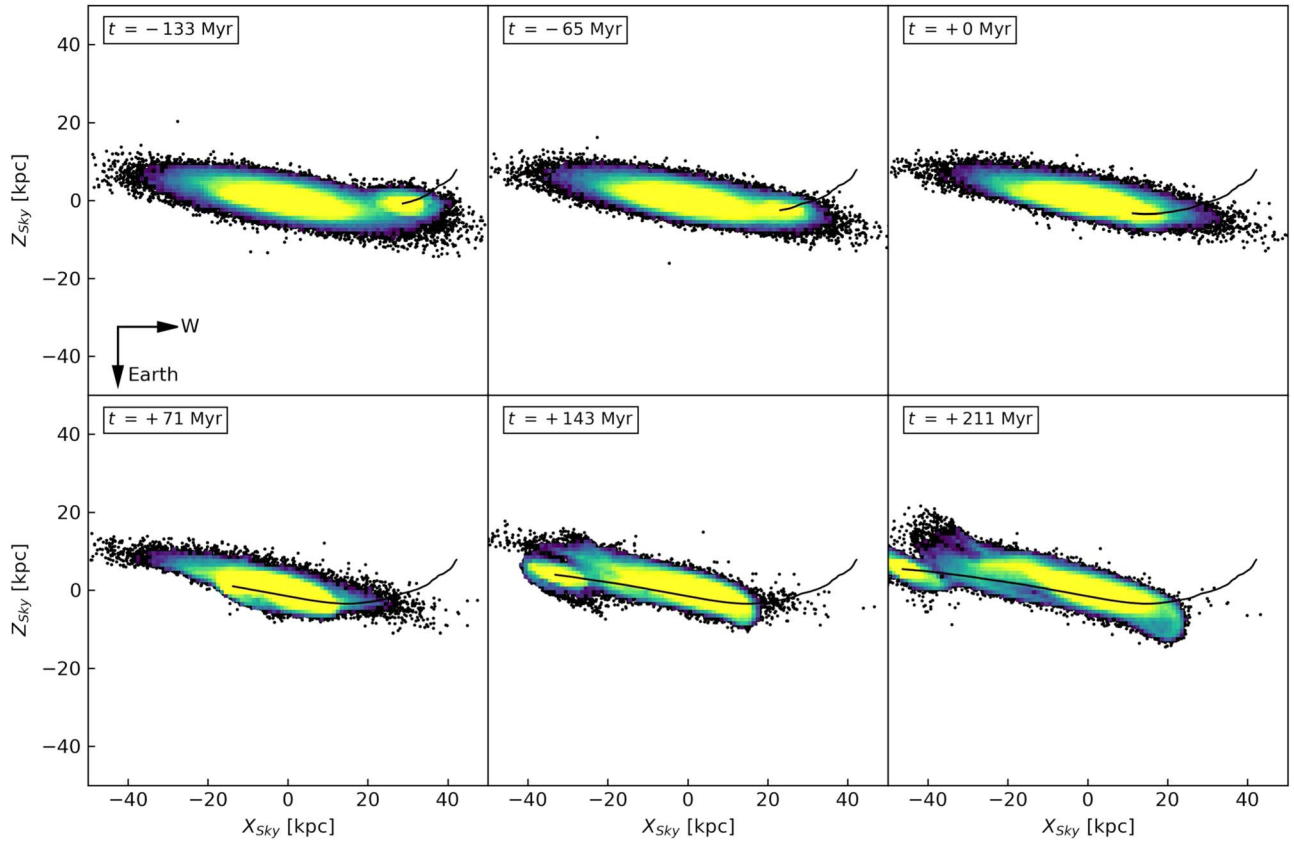


Figure 2. The M101/NGC 5474 simulation viewed orthogonal to the sky plane. Time is measured relative to the moment of periape ($t = 0$), with the last panel showing the current time. The simulation is visualized using a frame of reference that fixes M101 at the origin at all times, and NGC 5474’s orbital track is shown by the black line. An animation of this figure is available, showing the evolution of the interaction from $t = -269$ Myr to $t = +374$ Myr. The real-time duration of the animation is 24 s, and the animation pauses for 5 s at $t = +211$ Myr, the time of best match to the present-day M101 / NGC 5474 system.

(An animation of this figure is available.)

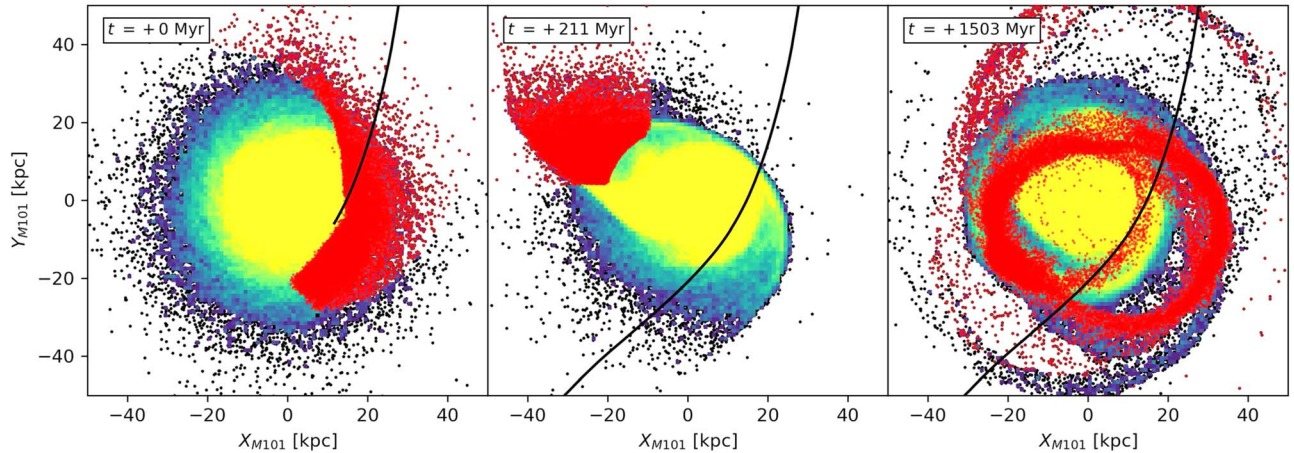


Figure 3. Zoomed-in view of the M101 disk at the moment of periape (left), the current time (center), and 1.3 Gyr in the future (right). NGC 5474’s orbital track is shown in black, and in each panel, particles found in today’s NE Plume are shown in red. At periape, material in the NE Plume was on the west side of M101, near the contact point of NGC 5474, but has since rotated around to form today’s NE Plume. In another gigayear, this material will have mixed azimuthally but remain in a coherent stream located in M101’s outer disk. An animation of this figure is available. The animation shows the evolution of M101’s disk from $t = -469$ Myr to $t = +2064$ Myr, with particles in today’s NE Plume shown in red. The real-time duration of the animation is 15 s.

(An animation of this figure is available.)

$32 \pm 11 \text{ km s}^{-1}$ (Zaritsky et al. 1990; Rownd et al. 1994). The model also has the sense of rotation in M101’s disk correct, with the north side being redshifted relative to systemic (Walter et al. 2008). More detailed kinematic matching to existing H I velocity data proves difficult, given that our simulation lacks

any hydrodynamic component. Nonetheless, some broad inferences are possible. Deep 21 cm mapping of the system (Huchtmeier & Witzel 1979; Mihos et al. 2012; Xu et al. 2021) has revealed H I between the two galaxies at intermediate velocities. Our model shows no similar stellar tidal bridge

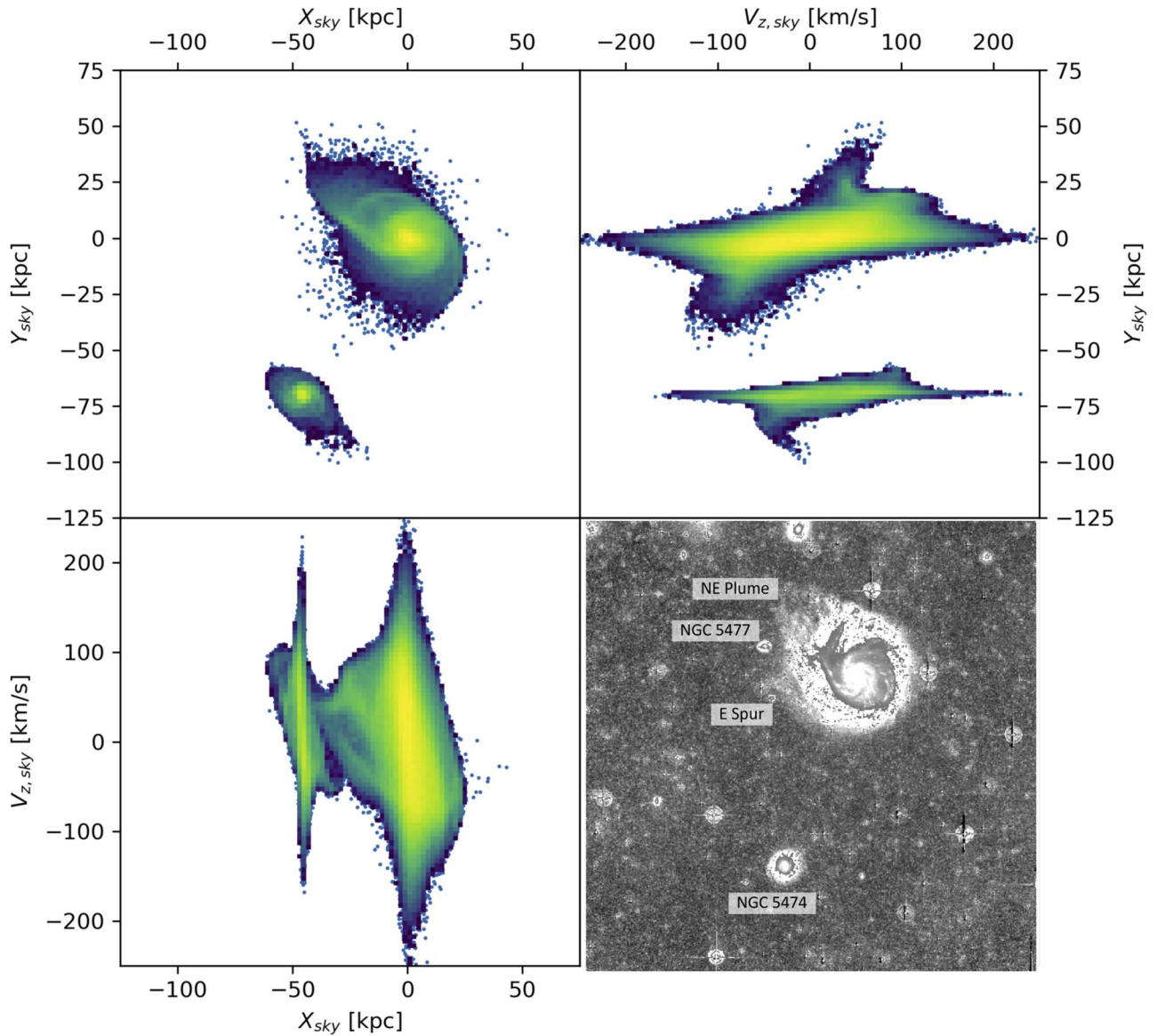


Figure 4. Position–velocity plots of the M101–NGC 5474 interaction model observed at the present time. The top left panel shows the sky view, while the top-right and lower-left panels show the model velocities collapsed along the X and Y coordinates, respectively. Radial velocity is measured relative to M101’s systemic velocity. The lower-right panel shows a deep B -band image of M101 from Mihos et al. (2013), with companion galaxies and tidal features marked.

linking the galaxies, which suggests the observed H I stream may be a result of ram pressure effects rather than simple tidal stripping. Similar arguments can be made regarding the high-velocity gas associated with the NE Plume (van der Hulst & Sancisi 1988; Walter et al. 2008), with velocities redshifted by $\gtrsim 100 \text{ km s}^{-1}$ compared to M101’s disk. We do see a spray of (collisionless) material in the NE Plume extending to higher velocity (Figure 4), which might plausibly be associated with that high-velocity cloud structure. This is material scattered out of the disk by NGC 5474’s passage, and ram pressure stripping might accentuate the structures seen here. However, at the moment of periape, the line-of-sight velocity of the companion as it impacted M101’s disk was only $\sim 60 \text{ km s}^{-1}$, significantly lower than the 100 km s^{-1} velocity spread of the high-velocity gas now seen in the NE Plume. It remains unclear, therefore, whether ram pressure effects could explain the full velocity range of the gas. Follow-up simulations that include hydrodynamics will be useful to test this aspect of the scenario.

4. Future Evolution

With M101’s encounter with NGC 5474 only $\sim 200 \text{ Myr}$ old—less than a single rotation period for M101’s outer disk—and its disk showing such strong, global asymmetry, the galaxy’s future evolution is very much an open question. Here we evolve the simulation forward in time to evaluate the effect of the encounter on M101’s long-term evolution. The encounter has led to only a modest amount of orbital decay in the system, leaving NGC 5474 on a very wide and loosely bound orbit that will not produce another close passage for many gigayears. Thus, over long timescales, M101’s further evolution is largely governed by its return to equilibrium after the initial perturbation of NGC 5474’s passage.

Figure 3(c) shows the M101 model approximately 1.3 Gyr after the impact. At this point, material in today’s NW Plume has wrapped completely around the galaxy, forming a coherent stream spanning a radial extent of $\approx 15\text{--}40 \text{ kpc}$. Given that the stellar population of the Plume is largely coeval (Mihos et al. 2018), the

stream will not only be kinematically coherent but also distinct in age and metallicity from the bulk of M101's stellar populations. Over time, this stream will continue to slowly mix radially and azimuthally in M101's outer disk, but—barring scattering or disruption by subsequent interactions (such as with the dwarf satellite NGC 5477)—will remain distinct in terms of its kinematics and stellar populations. Such a long-lived coherent stellar stream might be hard to distinguish from true accretion streams formed by the disruption of infalling satellite galaxies. Given the ubiquitous presence of star streams in the Milky Way and other spiral galaxies, it is possible that some of these observed streams may actually be due to original disk material “returning home” after a tidal encounter with a neighboring companion.

More globally, we can also examine changes in the radial distribution of stars in M101's disk. Disk galaxies often show differences in the radial scale length between the inner and outer disks, including both upbending ($h_{R,\text{outer}} > h_{R,\text{inner}}$) and downbending ($h_{R,\text{outer}} < h_{R,\text{inner}}$) radial profiles (e.g., Erwin et al. 2005; Pohlen & Trujillo 2006). Growing evidence links upbending profiles to galaxies in denser environments (Pohlen & Trujillo 2006; Watkins et al. 2019), suggesting interactions can either scatter disk material outwards or deposit accreted stars into a galaxy's outer disk. Mihos et al. (2012) showed that M101's surface brightness profile shows complex azimuthal variations (both downbending and upbending profiles) outside of a radius of $\approx 8'$ (16 kpc). That radius is similar to the pericenter distance of our encounter model (14 kpc), suggesting that the interaction is indeed reshaping M101's outer disk. If we measure the M101 disk profile at late times ($t \approx 1.5\text{--}2$ Gyr), after the present-day asymmetries have had time to mix azimuthally, we find evidence for spreading of the outer disk. Prior to the encounter, the disk had a uniform exponential profile with scale length $h_R = 4.4$ kpc, but at late times after the encounter, the disk shows an upbending profile with inner ($R < 15$ kpc) and outer ($R > 15$ kpc) scale lengths of $h_R = 4.2 \pm 0.1$ kpc and 5.3 ± 0.2 kpc, respectively. Thus, this interaction-driven reshaping of disk profiles may be a common evolutionary outcome in the loose group environment.

5. Summary and Future Directions

We have constructed the first N -body simulation to capture the gravitational encounter between M101 and its companion NGC 5474. The encounter involves a grazing, low-inclination passage of NGC 5474 through M101's outer disk ($R_{\text{peri}} \approx 14$ kpc), with the closest approach occurring approximately 200 Myr ago. The interaction was a retrograde passage for both galaxies, taking place largely in the plane of the sky as observed from our vantage point. Our simulation reproduces many of the features observed in the M101 system today: including the projected distance and velocity of the two galaxies, M101's overall lopsided asymmetry, the morphology of M101's NE spiral arm and NE Plume, and the sharp edge to the west side of M101's disk. We also roughly match the 200–300 Myr timescale for the encounter inferred from stellar age constraints in M101's NE Plume (Mihos et al. 2013, 2018) and show that this stellar population was likely formed in a burst of star formation triggered at the contact point when the two disks originally collided.

Evolving the system forward in time to evaluate the long-term evolution of M101, we find that no merger is imminent; NGC 5474 continues to move away from M101 on a wide and very loosely bound orbit, while the asymmetric structures currently seen in M101's disk slowly mix azimuthally as the

galaxy recovers from the collision. Material currently in M101's NE Plume falls back and wraps around the galaxy, resulting in a discrete stellar stream that is both phase-space coherent and coeval in age. At late times, M101's disk also shows an “upbending” surface density profile due to inner disk material drawn out by the interaction, similar to the upbending profiles often seen in disk galaxies found in dense group and cluster environments (Pohlen & Trujillo 2006; Watkins et al. 2019).

While our simulation reproduces many features of the M101 system, there remains room for improvement. First, our use of a collisionless simulation reproduces only the large-scale gravitational response to the encounter; adding gas physics to the simulation would let us examine the hydrodynamical response, including the detailed structure of the M101's spiral arms, the star-forming response of the disk, and the origin of M101's high-velocity gas. Second, further adjustments to the interaction model—such as a slower encounter velocity and a lower companion mass—might fix both our need for an overly massive model for NGC 5474 and the slight (~ 100 Myr) mismatch between the simulated collision time and the age of the post-starburst population in M101's outer disk. And finally, our simulation also ignores any role played by the dwarf galaxy NGC 5477. While this system is almost certainly too low mass to drive the large-scale asymmetry of M101, it could affect the outer disk morphology that constrains our model. Nonetheless, given the overall uncertainties, we find our interaction model to be a promising new description of M101's recent interaction history and its subsequent evolution.

The authors thank George Privon, Stacy McGaugh, and Ray Garner for help and encouragement over the course of this study.

ORCID iDs

Sean T. Linden  <https://orcid.org/0000-0002-1000-6081>
J. Christopher Mihos  <https://orcid.org/0000-0002-7089-8616>

References

- Bellazzini, M., Annibali, F., Tosi, M., et al. 2020, *A&A*, **634**, A124
Bosma, A., Goss, W. M., & Allen, R. J. 1981, *A&A*, **93**, 106
Erwin, P., Beckman, J. E., & Pohlen, M. 2005, *ApJL*, **626**, L81
Geller, M. J., & Huchra, J. P. 1983, *ApJS*, **52**, 61
Hernquist, L. 1987, *ApJS*, **64**, 715
Hernquist, L. 1990, *ApJ*, **356**, 359
Hernquist, L. 1993, *ApJS*, **86**, 389
Huchtmeier, W. K., & Witzel, A. 1979, *A&A*, **74**, 138
Kormendy, J., Drory, N., Bender, R., & Cornell, M. E. 2010, *ApJ*, **723**, 54
Mihos, J. C., Durrell, P. R., Feldmeier, J. J., Harding, P., & Watkins, A. E. 2018, *ApJ*, **862**, 99
Mihos, J. C., Harding, P., Spengler, C. E., Rudick, C. S., & Feldmeier, J. J. 2013, *ApJ*, **762**, 82
Mihos, J. C., Keating, K. M., Holley-Bockelmann, K., Pisano, D. J., & Kassim, N. E. 2012, *ApJ*, **761**, 186
Pascale, R., Bellazzini, M., Tosi, M., et al. 2021, *MNRAS*, **501**, 2091
Pohlen, M., & Trujillo, I. 2006, *A&A*, **454**, 759
Renaud, F., Athanassoula, E., Amram, P., et al. 2018, *MNRAS*, **473**, 585
Renaud, F., Boily, C. M., Naab, T., et al. 2009, *ApJ*, **706**, 67
Renaud, F., Bournaud, F., Kraljic, K., et al. 2014, *MNRAS*, **442**, 33
Rownd, B. K., Dickey, J. M., & Helou, G. 1994, *AJ*, **108**, 1638
Toomre, A., & Toomre, J. 1972, *ApJ*, **178**, 623
Tully, R. B. 1988, *Nearby galaxies catalog* (Cambridge: Cambridge Univ. Press)
van der Hulst, T., & Sancisi, R. 1988, *AJ*, **95**, 1354
Waller, W. H., Bohlin, R. C., Cornett, R. H., et al. 1997, *ApJ*, **481**, 169
Walter, F., Brinks, E., de Blok, W. J. G., et al. 2008, *AJ*, **136**, 2563
Watkins, A. E., Laine, J., Comerón, S., et al. 2019, *A&A*, **625**, A36
Xu, J.-L., Zhang, C.-P., Yu, N., et al. 2021, *ApJ*, **922**, 53
Zaritsky, D., Elston, R., & Hill, J. M. 1990, *AJ*, **99**, 1108